Investigation of whether in-room CT-based adaptive intracavitary brachytherapy for uterine cervical cancer is robust against interfractional location variations of organs and/or applicators

奥, 好史

https://doi.org/10.15017/1670404

出版情報：九州大学, 2016, 博士（保健学）, 課程博士
バージョン：
権利関係：全文ファイル公表済

Journal of Radiation Research Advance Access published June 13, 2016

Journal of Radiation Research, 2016, pp. 1–7
doi: 10.1093/jrr/rrw043
Regular Paper

Investigation of whether in-room CT-based adaptive intracavitary brachytherapy for uterine cervical cancer is robust against interfractional location variations of organs and/or applicators

Yoshifumi Oku[1,2], Hidetaka Arimura[3]*, Tran Thi Thao Nguyen[1], Yoshiyuki Hiraki[4], Masahiko Toyota[5], Yasumasa Saigo[5], Takashi Yoshiura[6] and Hideki Hirata[3]

[1]Department of Health Sciences, Graduate School of Medical Sciences, Kyushu University, 3-1-1 Maidashi, Higashi-ku, Fukuoka 812-8582, Japan
[2]Division of Radiology, Department of Medical Technology, Kyushu University Hospital, 3-1-1 Maidashi, Higashi-ku, Fukuoka 812-8582, Japan
[3]Department of Health Sciences, Faculty of Medical Sciences, Kyushu University, 3-1-1, Maidashi, Higashi-ku, Fukuoka 812-8582, Japan
[4]Department of Radiation Oncology, Fujimoto General Hospital, 17-1 Hayasuzucho, Miyakonojo, Miyazaki 885-0055, Japan
[5]Division of Radiology, Department of Clinical Technology, Kagoshima University Hospital, 8-35-1 Sakuragaoka, Kagoshima, Kagoshima 890-0075, Japan
[6]Graduate School of Medical and Dental Sciences, Kagoshima University, 8-35-1 Sakuragaoka, Kagoshima, Kagoshima 890-0075, Japan
*Corresponding author. Division of Quantum Radiation Science, Department of Health Sciences, Faculty of Medical Sciences, Kyushu University, 3-1-1, Maidashi, Higashi-ku, Fukuoka 812-8582, Japan. Tel and Fax: +81-92-642-6719; Email: arimurah@med.kyushu-u.ac.jp
Received December 1, 2015; Revised February 3, 2016; Accepted March 23, 2016

ABSTRACT

This study investigates whether in-room computed tomography (CT)-based adaptive treatment planning (ATP) is robust against interfractional location variations, namely, interfractional organ motions and/or applicator displacements, in 3D intracavitary brachytherapy (ICBT) for uterine cervical cancer. In ATP, the radiation treatment plans, which have been designed based on planning CT images (and/or MR images) acquired just before the treatments, are adaptively applied for each fraction, taking into account the interfractional location variations. 2D and 3D plans with ATP for 14 patients were simulated for 56 fractions at a prescribed dose of 600 cGy per fraction. The standard deviations (SDs) of location displacements (interfractional location variations) of the target and organs at risk (OARs) with 3D ATP were significantly smaller than those with 2D ATP ($P < 0.05$). The homogeneity index (HI), conformity index (CI) and tumor control probability (TCP) in 3D ATP were significantly higher for high-risk clinical target volumes than those in 2D ATP. The SDs of the HI, CI, TCP, bladder and rectum D_{2cc}, and the bladder and rectum normal tissue complication probability (NTCP) in 3D ATP were significantly smaller than those in 2D ATP. The results of this study suggest that the interfractional location variations give smaller impacts on the planning evaluation indices in 3D ATP than in 2D ATP. Therefore, the 3D plans with ATP are expected to be robust against interfractional location variations in each treatment fraction.

KEYWORDS: interfractional location variation, robustness, adaptive intracavitary brachytherapy, planning evaluation indices, in-room computed tomography

INTRODUCTION

Intracavitary brachytherapy (ICBT) plays an essential role in definitive radiotherapy for cervical cancer [1, 2]. In ICBT, an applicator is inserted into the body cavity and, subsequently, a radioactive source is fed into the applicator to intensively irradiate the target tumor.

In general, ICBT employs point-based and volume-based treatment planning approaches, namely, 2D and 3D approaches. Point A

and International Commission of Radiation Units and Measurements (ICRU) organs at risk (OAR) (bladder and rectum) points have been conventionally used in 2D ICBT planning based on 2D X-ray projection images, as this approach is practically simple and convenient [3]. However, Brooks *et al.* reported that the D_{2cc} rectal dose was higher for the ICRU rectal point for both conformal and standard plans, but the bladder ICRU point underestimated the dose [4].

On the other hand, a prescribed dose of D90 for cervical tumors and D_{2cc} for OARs have been employed in the volume-based ICBT planning based on 3D images, such as computed tomography (CT), magnetic resonance (MR) [5] and positron emission tomography (PET) images [6]. The Groupe Européen de Curiethérapie (GEC) and the European Society for Radiotherapy & Oncology (ESTRO) (GEC-ESTRO) working group have published recommendations including concepts, terms and pitfalls in 3D-image–based ICBT for cervical cancer [7–9]. A number of studies recommend D90, which is defined as the minimum dose delivered to 90% of the high-risk clinical target volume (HR-CTV), with a correlation with the regional tumor control rate, as a better dose index than point A [10–12]. Furthermore, D_{2cc} for the bladder and rectum, which were defined as the minimum doses delivered to 2 cc of the organ volume receiving the most intense irradiation, are useful indicators of toxicity [13].

ICBT suffers from several critical problems, particularly interfractional organ motions during treatment courses. The OARs adjacent to the target tumor, such as the bladder, rectum, sigmoid colon, and small intestine, are irradiated because of intra- and interfractional organ motions, which can result in late radiation damage to the OAR in some cases [14]. In addition, 2D planning could also lead to uncertainty regarding whether entire cervical tumors are covered with the prescribed isodose surface of point A dose [15], especially when interfractional organ motions occur. Another problem encountered is applicator displacements from the planned positions. Schindel *et al.* reported that applicator displacements caused a dosimetric change of greater than 10% in both 2D and 3D plans [16] when the displacements in simulated planning studies were ±3 mm at applicator reconstruction uncertainties of ±4.5 mm. The above results suggest that ICBT is sensitive to interfractional organ motions and/or applicator displacements, which could result in lowering of treatment outcomes. Consequently, adaptive treatment planning (ATP) based on 3D CT and/or MR images for each fraction has attracted increasing attention in ICBT [17, 18].

In ATP, radiation treatment plans, which have been designed based on planning CT images (and/or MR images) acquired just before the treatments, are adaptively applied for each fraction, taking into account the interfractional location variations. Kirisits *et al.* compared dose evaluation indices between the MR-based 3D ATP and single MR-based treatment planning for cervical cancer brachytherapy [19]. The use of only one MR-based treatment plan resulted in a higher dose to OAR structures, and thus the MR-based ATP can help to reduce certain situations of overdosage. Hellebust *et al.* quantified interfractional variations of doses to critical organs for patients receiving ICBT, by using an *in situ* CT scanner after each treatment fraction [20]. According to their results, a CT examination should be provided at every fraction, although they did not employ the ATP strategy.

To the best of our knowledge, no studies comparing ICBT with 2D and 3D ATP have yet been conducted to investigate whether 3D ATP is robust against interfractional location variations of organs and/or applicators. Therefore, in this study we investigated the robustness of 3D ATP for cervical cancer by measuring planning evaluation indices and locations for the target and OARs, and their interfractional location variations for ICBT with 2D and 3D ATP. The interfractional location variations in all treatment fractions were evaluated as location displacements by measuring the 3D coordinates of point A for the target, ICRU reference point for OARs (bladder and rectum) in the 2D plan, and centroids of the clinical target volume (CTV) and OARs in the 3D plan. Furthermore, the planning evaluation indices were the homogeneity index (HI), conformity index (CI), tumor control probability (TCP) for a high-risk clinical target volume (HR-CTV), as well as ICRU doses, D_{2cc}, and normal tissue complication probability (NTCP) for the bladder and rectum.

MATERIALS AND METHODS

Clinical cases

The institutional review board (IRB) of our university hospital approved this retrospective study. Table 1 shows the patient characteristics of the cases investigated in the study. A total of 56 fractions from 14 patients (age range: 29–73 years; median: 63 years) with cervical cancer, who received ICBT between January 2011 and March 2013, were selected for this study under the protocol approved by the IRB. For all of the patients, squamous cell carcinoma was found to be the predominant histological type of uterine cervix carcinoma. The tumor stages were determined according to the International Federation of Gynecology and Obstetrics classification as Stage Ib2 for nine patients, Stage IIa for four patients, and Stage IIb for one patient. The total prescribed dose for each patient was 2400 cGy (600 cGy/fraction) at the target for four fractions.

Overall treatment procedures for ICBT with ATP

The 2D and 3D treatment plans with ATP were simulated for 14 patients to investigate the impact of ATP in ICBT. In 2D or 3D ATP, the radiation treatment plans were adaptively designed for the treatments in all of the fractions according to the X-ray projection images (2D ATP) or planning CT images acquired just before the treatments and the first MR image (3D ATP).

Table 1. Patient characteristics for the 14 cases used in this study

Characteristics		Median	Range	Total (*n*)
Patient's age (years)		63	29–73	14
Histologic type	Squamous cell carcinoma			14
FIGO stage	Ib			9
	IIa			4
	IIb			1

Two experienced radiation oncologists designed the 2D and 3D plans for application to a radiation treatment planning (RTP) system (OncentraBrachy version 4.3; Nucletron, an Elekta company, Netherlands). A CT/MRI-compatible applicator (Fletcher CT/MR Applicator Set, part# 189.730; Nucletron, an Elekta company, Netherlands) consisting of uterine tandems of various lengths and two ovoids was employed for all patients.

2D treatment plans

The 2D plans were designed based on Manchester point A and ICRU OARs points. X-ray images of the anterior–posterior (AP) and lateral views for patients in the lithotomy position were acquired by using a mobile C-arm X-ray system (Siremobile Compact L; Siemens, Germany) at an X-ray tube voltage of 90 kV and a tube current of 20 mAs after inserting the applicator. The image data were transferred to an RTP system (OncentraBrachy version 4.3; Nucletron, an Elekta company, Netherlands). Point A was defined as the location 2 cm lateral to the central canal of the uterus and 2 cm above the mucous membrane of the lateral fornix, along the axis of the uterus [3]. The bladder ICRU reference point was localized by using a Foley catheter (2-Way Silicone-Elastomer Foley catheter II, Toray Medical Co., Tokyo, Japan), with a balloon filled with 7 cc of a radiopaque fluid, and the rectal ICRU reference point was determined on a line drawn from the midpoint of the activity in the ovoids, 5 mm behind the posterior vaginal wall [3]. Point A, the ICRU bladder and rectum reference points, source track, and dwell positions were digitally localized on the AP- and lateral-view images, and the data were transferred to the RTP system. The applicator was reconstructed based on this information. The dwell times of all sources were determined using a dose point optimization method. In each 2D plan, a prescribed dose of 600 cGy was applied to left and right points A, while minimizing the OARs doses at the ICRU bladder and rectum reference points. These procedures were performed for each fraction.

3D treatment plans

All patients in the lithotomy position, with applicators inserted in their bodies, were scanned using a 20-slice CT scanner (Somatom Sensation; Siemens, Germany) with a matrix size of 512 × 512, a pixel size of 0.68 mm in the *x*–*y* plane, and a slice thickness of 2.0 mm, at an X-ray tube voltage of 120 kV and a tube current of 300 mAs. The image data were transferred to the RTP system.

A T2-weighted MR image was acquired once for each patient with a pelvic surface coil by using a 3.0-Tesla MR scanner (Magnetom Trio; Siemens, Germany) with a matrix size of 512 × 512, an in-plane pixel size of 0.47, and a slice thickness of 5 mm without a slice gap. The axial images were obtained from the level above the uterine fundus to the inferior border of the symphysis pubis below any vaginal tumor extension, and sagittal images were obtained from locations between the internal obturator muscles.

The HR-CTV does not include any safety margins and consists of the residual tumor at the time of brachytherapy, presumed as palpable and visible by clinical examination and as detectable on MRI (areas of high-signal intensity in T2-weighted images). Gray zones in the parametria expanding in the direction of the initial tumor spread appear on the T2-weighted images as areas of intermediate signal intensity. These gray zones are also assumed to be highly susceptible to residual disease, indicating a high risk of disease recurrence, and are therefore included in the HR-CTV [5, 6]. The D_{2cc} for the bladder and rectum was defined as the minimum dose delivered to 2 cc of the organ volume receiving the most intense irradiation. The contours of the HR-CTV, bladder and rectum regions were delineated based on a consensus between a radiation oncologist and medical physicist on the CT images together with fusion images with the first T2-weighted MR image, according to the recommendations of the GEC-ESTRO [7–9]. A fusion image obtained from an MR image and a planning CT image for each fraction was produced by using a manual registration based on mutual information within a rectangular volume of interest (VOI), which was manually determined. The 3D plans were optimized so that D90 could be maintained at a prescribed dose of 600 cGy.

Location displacements of targets and OARs in each treatment fraction

The location displacements of the target and OARs in all treatment fractions were evaluated by measuring the 3D coordinates of point A, ICRU reference point for OARs (bladder and rectum) based on the AP- and lateral-view images in the 2D plan, and centroids of the HR-CTV and the OARs based on 3D CT images in the 3D plan. The location displacements were determined as Euclidean distances between two position vectors of the objective points for the first and other fractions. The Euclidean distance d was calculated by the following equation:

$$d = ||r_1 - r_i||, \quad (1)$$

where $||\bullet||$ represents the Euclidean distance, r_1 is the position vector for the first fraction, and r_i is the position vector in the ith fraction.

Treatment planning evaluation indices

The HI, CI and TCP were measured as the planning evaluation indices for the HR-CTV, and ICRU reference doses, D_{2cc} and NTCP for the OARs. The HI, which is defined as the ratio of the maximum dose to the minimum dose in the HR-CTV, represents the dose uniformity in a target volume [21]. The CI, which is defined as the ratio of the treated volume to the HR-CTV, represents the degree of conformity. In this study, the treated volume was defined as the volume receiving the minimum dose in the HR-CTV [22]. The HI and CI are 1.0 (minimum value) for an ideal case, but they would be larger than 1.0 for general cases. The dose index was used as a tool to define the quality of the treatment plans, considering both target coverage and the degree of normal tissue irradiation [23].

The TCP was estimated using a linear–quadratic (LQ) model according to a Poisson distribution by considering the radiosensitivity variation and non-uniform dose distribution [24]. The TCP averaged over the population with variable radiosensitivity, which was simulated as a Gaussian distribution of α_k values with a

mean α and a standard deviation σ_α in K groups of patients, is given by:

$$TCP = \sum_{k=1}^{K} \left(\frac{1}{\sqrt{2\pi}\,\sigma_\alpha} \right) \exp\left\{ -\frac{(\alpha_k - \bar{\alpha})^2}{2\sigma_\alpha^2} \right\} \times \prod_{l=1}^{L} \exp\left[-\rho_c v_l \bullet \exp\left\{ -\alpha_k D_l \left(1 + \frac{d_l}{\alpha_k/\beta_k} \right) \right\} \right], \quad (2)$$

where k is the group number, ρ_c is the number of initial clonogenic cells per cubic centimeter, L is the number of dose bins of the differential DVH in the HR-CTV, l is lth voxel, vl is the volume (cm^3) irradiated by a dose d_l (Gy) per fraction in the HR-CTV, and D_l is the total dose (Gy) at v_l. α_k ranged from α-$3\sigma_\alpha$ to α+$3\sigma_\alpha$, which was divided by K. Moreover, the NTCP for the bladder and rectum were calculated by using the Lyman–Kutcher–Burman model [25–27]. For the calculation of the NTCP, the dose scale of a DVH was re-scaled as an LQ equivalent dose (LQED) for 2 Gy fractions as follows:

$$LQED = D\frac{\alpha/\beta + d}{\alpha/\beta + 2}, \quad (3)$$

where D is the total dose (Gy), d is the dose per fraction (Gy) at D in the differential DVH, and α, and β are cellular radiosensitivity LQ parameters. Then, the NTCP was calculated by:

$$NTCP = \frac{1}{\sqrt{2\pi}} \int_{-\infty}^{t} \exp\left(-\frac{x^2}{2} \right) dx = \frac{1}{2}\left\{ 1 + \mathrm{erf}\left(\frac{t}{\sqrt{2}} \right) \right\}, \quad (4)$$

$$t = \frac{LQED_{max} - TD_{50}(v)}{mTD_{50}(v)}, \quad (5)$$

$$v = \frac{v_{eff}}{v_{ref}}, \quad (6)$$

$$v_{eff} = \sum_{j=1}^{N} \left(\frac{LQED_j}{LQED_{max}} \right)^{1/n} v_j, \quad (7)$$

$$TD_{50}(v) = TD_{50}(v_{ref}) \bullet v^{-n}, \quad (8)$$

where $TD_{50}(v)$ and $TD_{50}(v_{ref})$ are the tolerance doses (Gy) that cause a 50% complication rate within 5 years after treatment for uniform irradiation of the partial volume v according to Eqs (6) and (8), and reference volume v_{ref}, respectively. The parameters n and m control the volume effect and the slope of the dose–response curve, respectively. By using an effective volume method [24], a non-uniform dose distribution, which has a volume bin v_j with a dose of $LQED_j$ in the differential DVH, was transformed into a uniform dose distribution with an effective volume v_{eff} at the maximum dose of $LQED_{max}$ in Eq. (7). In this study, α/β was set as 10 Gy for the target, and 3.0 Gy for the bladder and rectum [9] in the LQ model. The fitting parameter values n, m and $TD_{50}(v_{ref})$ were set at 0.13, 0.11 and 90 Gy for the bladder, and at 0.06, 0.15 and 75 Gy for the rectum, respectively; these values were obtained from the report of Burman *et al.* [25, 28].

Statistical analysis

The means and standard deviations (SDs) of the location displacements and planning evaluation indices of the target and OARs between the 2D and 3D plans were evaluated by using a Welch *t*-test and *F*-test, respectively. The difference was considered statistically significant when the *P* value was smaller than 0.05.

RESULTS

Table 2 shows the means and standard deviations of location displacements (interfractional location variations) of targets and OARs, which were evaluated by point A and the centroid of the HR-CTV, and ICRU reference points and the centroids of the D_{2cc} for the bladder and rectum, in 56 treatment plans for 14 cases evaluated using the RTP system in the 2D and 3D plans with ATP. Figure 1 shows the location displacements of target, bladder and rectum, which are the same data as presented in Table 2. The mean location displacements of the target and OARs for the bladder and rectum did not exhibit any statistically significant difference in any of the treatments ($P > 0.05$). However, the SDs of the location displacements in 3D plans with ATP were significantly smaller in the Euclidean distance than those in 2D ATP ($P < 0.05$). These results indicate that the precision of the 3D ATP was higher than that of the 2D ATP.

Table 3 shows means ± SDs of the planning evaluation indices, i.e. the HI, CI and TCP for the HR-CTV, and ICRU doses, D_{2cc} and NTCPs for the bladder and rectum, which were obtained from the dose distributions produced by the 2D and 3D plans for 56 fractions in 14 cases. Figure 2 shows bar graphs of the HI and CI for HR-CTV. The HI and CI for the 3D ATP were significantly smaller than those for 2D ATP ($P < 0.05$). A smaller HI or CI implies better homogeneity and conformity indices. It can be seen from Fig. 3 that the TCP for 3D ATP is significantly greater than that for 2D ATP ($P < 0.05$). These results denote that the degrees of homogeneity, conformity and TCP for 3D ATP were significantly better with respect to the HR-CTV than those for 2D ATP. The SDs of the HI, CI and TCP for 3D ATP were significantly smaller than those

Table 2. Means and standard deviations of location displacements (mm) of targets and OARs in 56 treatment plans for 14 cases evaluated from a radiation treatment planning system in 2D and 3D plans with ATP

Organ	2D plan Point A for the target; ICRU reference point for OARs	3D plan Centroid of HR-CTV and OARs
Target	2.99 ± 1.80	2.80 ± 1.11
OAR		
Bladder	4.22 ± 2.05	3.80 ± 1.50
Rectum	4.00 ± 1.91	3.70 ± 1.30

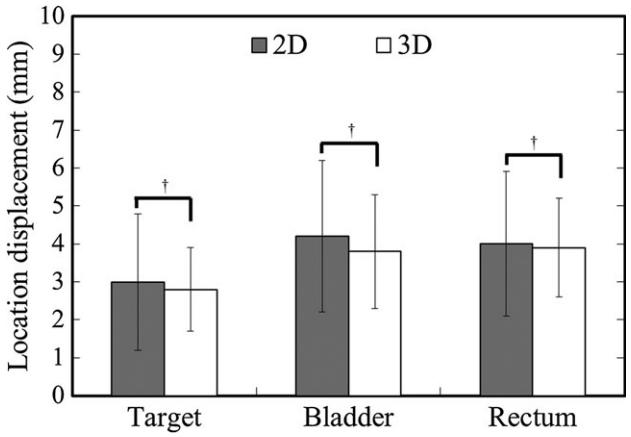

Fig. 1. Location displacements of targets and OARs, which were evaluated by point A and the centroid of the HR-CTV, and ICRU reference points and the centroids of the D_{2cc} for the bladder and rectum, for 2D (gray) and 3D (white) ATP. The error bars indicate standard deviations, and a dagger indicates statistical significance ($P < 0.05$) for the standard deviation, respectively.

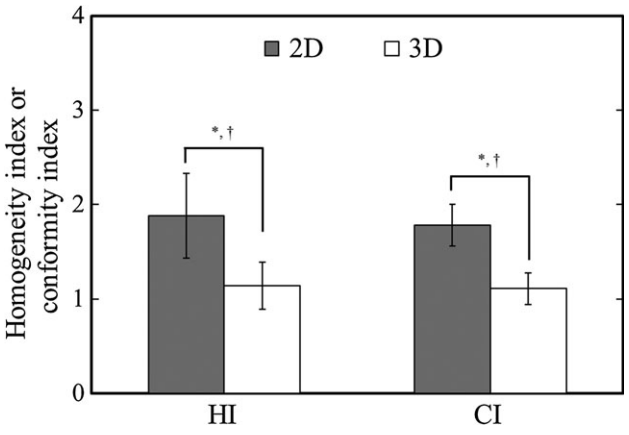

Fig. 2. Homogeneity index and conformity index for 2D (gray) and 3D (white) ATP. The error bars indicate standard deviations, and an asterisk and dagger indicate statistical significance ($P < 0.05$) for the mean and standard deviation, respectively.

Table 3. Means and standard deviations of planning evaluation indices in 56 treatment plans for 14 cases obtained from dose distributions in 2D and 3D plans with ATP[a]

Planning evaluation index	2D plan (Point A = 600 cGy)	3D plan (D90 = 600 cGy)
Target		
Homogeneity index	1.88 ± 0.45	1.14 ± 0.21
Conformity index	1.78 ± 0.31	1.11 ± 0.20
TCP[b] (%)	96.0 ± 1.52	98.9 ± 0.23
OAR		
ICRU bladder dose (cGy)	326 ± 42.2	315 ± 45.4
D_{2cc} bladder dose (cGy)	356 ± 51.2	381 ± 31.5
ICRU rectum dose (cGy)	301 ± 26.1	310 ± 29.4
D_{2cc} rectum dose (cGy)	297 ± 42.0	323 ± 29.9
NTCP[c] of bladder (%)	20.6 ± 7.19	18.4 ± 5.02
NTCP of rectum (%)	12.1 ± 8.03	13.9 ± 4.75

[a]ATP = adaptive treatment planning.
[b]TCP = tumor control probability.
[c]NTCP = normal tissue complication probability.

for 2D ATP ($P < 0.05$). According to these results, 3D ATP is more precise or robust in terms of dose delivery to the HR-CTV, even if interfractional location variations occur in treatment sessions, as shown in Table 2 and Fig. 1.

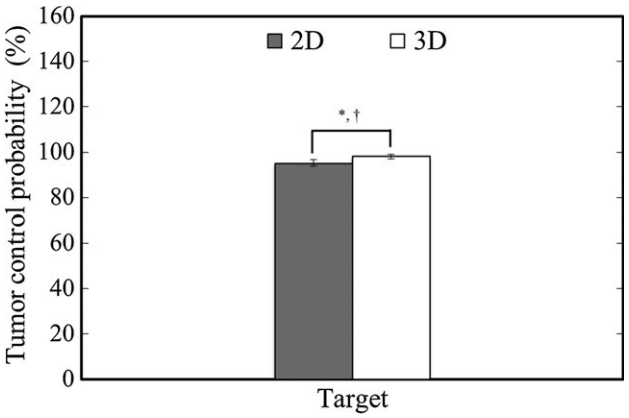

Fig. 3. Tumor control probability for 2D (gray) and 3D (white) ATP. The error bars indicate standard deviations, and an asterisk and dagger indicate statistical significance ($P < 0.05$) for the mean and standard deviation, respectively.

Figures 4 and 5 show the bar graphs of the ICRU doses and D_{2cc} for the bladder and rectum, respectively. The results show no significant differences between the two methods in terms of the average values of ICRU doses and D_{2cc}. The figures indicate that 3D ATP is equivalent to 2D ATP in terms of dose distributions on the OARs. The SDs of D_{2cc} for the bladder and rectum in 3D ATP were smaller than those in 2D ATP ($P < 0.05$).

Figure 6 shows the bar graphs of the NTCPs of the bladder and rectum for 2D and 3D ATP. In Figure 6, it can be seen that there are no statistically significant differences in the NTCPs for the bladder and rectum between the two methods, whereas the SDs for the bladder and rectum in 3D ATP were significantly smaller than those in 2D ATP ($P < 0.05$).

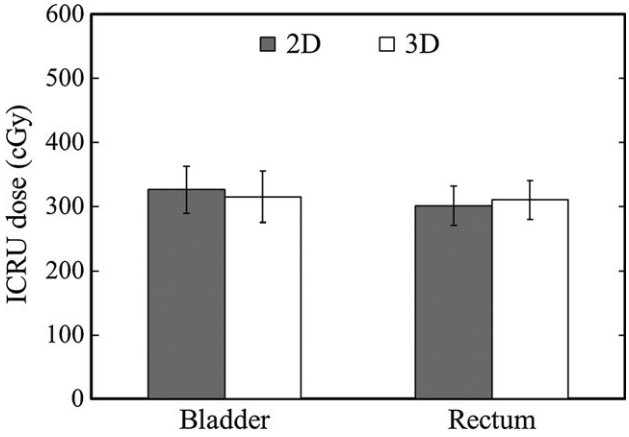

Fig. 4. ICRU bladder and rectum dose for 2D (gray) and 3D (white) ATP. The error bars indicate standard deviations.

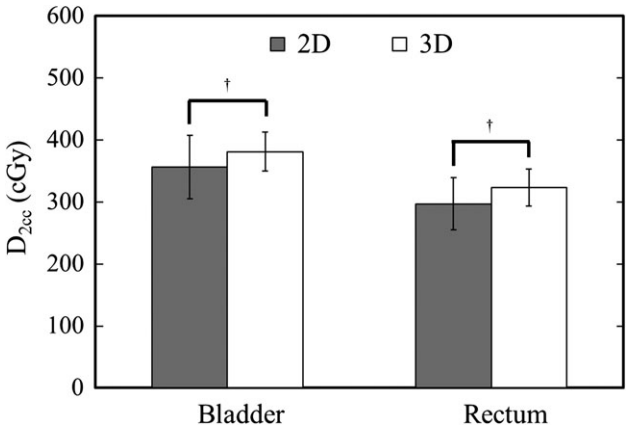

Fig. 5. Bladder and rectum D_{2cc} for 2D (gray) and 3D (white) ATP. The error bars indicate standard deviations, and a dagger indicates statistical significance ($P < 0.05$) for the standard deviation, respectively.

DISCUSSION

In this study, we investigated the robustness of 3D ATP in ICBT against interfractional location variations, that is, interfractional organ motions and/or applicator displacements. The interfractional location variation results show that the uncertainty of 3D ATP was smaller than that of 2D ATP. Assuming that the displacements of point A represent those of the tandem, no significant difference was observed in the average location displacements of the tandem between 2D and 3D ATP, but the SDs of the HI, CI and TCP for 3D ATP were significantly smaller than those for 2D ATP. This indicates that 3D ATP has robust planning evaluation indices against tandem displacements.

This study demonstrated that the SDs of the HI, CI, TCP and D_{2cc} for the bladder and rectum, and the bladder and rectum NTCPs for 3D ATP were significantly smaller than those for 2D ATP. In addition, 3D ATP could provide better dose distributions for the HR-CTV by increasing the precision of dose delivery to the HR-CTV and reducing the dose to OARs in ICBT. Thus, it is clear that interfractional location variations have a larger impact on the planning evaluation indices in 2D ATP than in 3D ATP. Therefore, 3D ATP is expected to be robust against interfractional location variations.

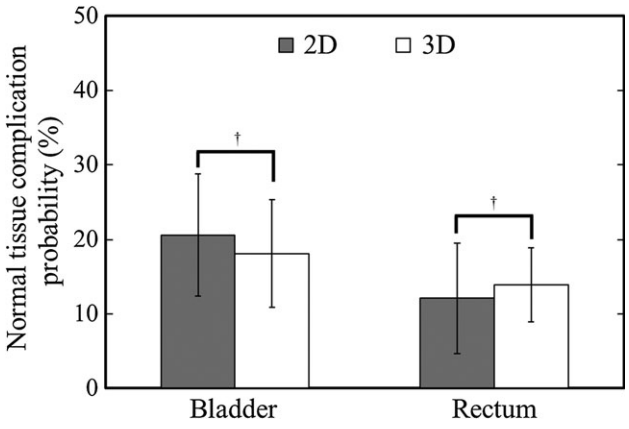

Fig. 6. NTCP of the bladder and rectum for 2D (gray) and 3D (white) ATP. The error bars indicate standard deviations, and a dagger indicates statistical significance ($P < 0.05$) for the standard deviation, respectively.

CONCLUSIONS

We investigated the robustness of 3D ATP against interfractional location variations of organs and applicators for cervical cancer by measuring their locations and planning evaluation indices for targets and OARs, and the corresponding deviations for ICBT with 2D and 3D ATP. The results indicate that interfractional location variations have a smaller impact on the planning evaluation indices in 3D ATP compared with those in 2D ATP. Therefore, it is inferred that the 3D plan with ATP is robust against interfractional location variations in each treatment fraction.

There are two main limitations in this study. First, the prognoses for the 14 patients considered in this study have not been evaluated due to the short-term experience of ICBT with ATP in our institution. Second, only cases at Stages Ib ($n = 9$), IIa ($n = 4$), and IIb ($n = 1$) were included in this study, and thus a larger database including a greater range of stages should be analyzed to strengthen the statistical nature of the conclusions drawn in this study.

ACKNOWLEDGEMENTS

The authors would like to express our gratitude to all members in Arimura laboratory (http://web.shs.kyushu-u.ac.jp/~arimura/) for insightful comments and suggestions.

FUNDING

This research was partially supported by the JSPS KAKENHI Grant no. 26670301 (Grant-in-Aid for Challenging Exploratory Research).

CONFLICT OF INTEREST

The authors declare that there are no conflicts of interest.

REFERENCES

1. Park HC, Suh CO, Kim GE. Fractionated high-dose-rate brachytherapy in the management of uterine cervical cancer. *Yonsei Med J* 2002;43:737–48.
2. Nori D, Dasari N, Allbright RM. Gynecologic brachytherapy I: proper incorporation of brachytherapy into the current multimodality management of carcinoma of the cervix. *Semin Radiather Oncol* 2002;12:40–52.
3. International Commission on Radiation Units and Measurements (ICRU). Dose and volume specification for reporting intracavitary therapy in gynecology. *ICRU Report 38*. Bethesda, MD: ICRU, 1985.
4. Brooks S, Bownes P, Lowe G, et al. Cervical brachytherapy utilizing ring applicator: comparison of standard and conformal loading. *Int J Radiat Oncol Biol Phys* 2005;63:934–39.
5. Dolezel M, Odrazka K, Vanasek J, et al. MRI-based pre-planning in patients with cervical cancer treated with three-dimensional brachytherapy. *Br J Radiol* 2011;84:850–56.
6. Lin LL, Mutic S, Low DA, et al. Adaptive brachytherapy treatment planning for cervical cancer using FDG–PET. *Int J Radiat Oncol Biol Phys* 2007;67:91–6.
7. Haie-Medar C, Pötter R, Limbergen EV, et al. Recommendations from Gynaecological (GYN) GEC-ESTRO Working Group (I): concepts and terms in 3D image based 3D treatment planning in cervix cancer brachytherapy with emphasis on MRI assessment of GTV and CTV. *Radiother Oncol* 2005;74:235–45.
8. Pötter R, Haie-Meder C, Limbergen EV, et al. Recommendations from Gynaecological (GYN) GEC-ESTRO Working Group (II): concepts and terms in 3D image-based treatment planning in cervix cancer brachytherapy—3D dose volume parameters and aspects of 3D image-based anatomy, radiation physics, radiobiology. *Radiother Oncol* 2006;78:67–77.
9. Hellebust TP, Kirisits C, Berger D, et al. Recommendations from Gynaecological (GYN) GEC-ESTRO Working Group: considerations and pitfalls in commissioning and applicator reconstruction in 3D image-based treatment planning of cervix cancer brachytherapy. *Radiother Oncol* 2010;96:153–60.
10. Dimopoulos JC, Lang S, Kirisits C, et al. Dose–volume histogram parameters and local tumor control in magnetic resonance image-guided cervical cancer brachytherapy. *Int J Radiat Oncol Biol Phys* 2009;75:56–63.
11. Pötter R, Georg P, Dimopoulos JC, et al. Clinical outcome of protocol based image (MRI) guided adaptive brachytherapy combined with 3D conformal radiotherapy with or without chemotherapy in patients with locally advanced cervical cancer. *Radiother Oncol* 2011;100:116–23.
12. Schmid MP, Kirisits C, Nesvacil N, et al. Local recurrences in cervical cancer patients in the setting of image-guided brachytherapy: a comparison of spatial dose distribution within a matched-pair analysis. *Radiother Oncol* 2011;100:468–72.
13. Kirisits C, Pötter R, Lang S, et al. Dose and volume parameters for MRI-based treatment planning in intracavitary brachytherapy for cervical cancer. *Int J Radiat Oncol Biol Phys* 2005;62:901–11.
14. Nakano T, Kato S, Ohno T, et al. Long-term results of high-dose rate intracavitary brachytherapy for squamous cell carcinoma of the uterine cervix. *Cancer* 2005;103:92–101.
15. Ohkubo Y, Ohno T, Noda SE, et al. Interfractional change of high-risk CTV D90 during image-guided brachytherapy for uterine cervical cancer. *J Radiat Res* 2013;54:1138–45.
16. Schindel J, Zhang W, Bhatia SK, et al. Dosimetric impacts of applicator displacements and applicator reconstruction-uncertainties on 3D image-guided brachytherapy for cervical cancer. *J Contemp Brachytherapy* 2013;5:250–57.
17. Pötter R, Fidarova E, Kirisits C, et al. Image-guided adaptive brachytherapy for cervix carcinoma. *Clin Oncol* 2008;20:426–32.
18. Pötter R, Kirisits C, Fidarova EF, et al. Present status and future of high-precision image guided adaptive brachytherapy for cervix carcinoma. *Acta Oncol* 2008;47:1323–36.
19. Kirisits C, Lang S, Dimopoulos J, et al. Uncertainties when using only one MRI-based treatment plan for subsequent high-dose-rate tandem and ring applications in brachytherapy of cervix cancer. *Radiother Oncol* 2006;81:269–75.
20. Hellebust TP, Dale E, Skjønsberg A, et al. Inter fraction variations in rectum and bladder volumes and dose distributions during high dose rate brachytherapy treatment of the uterine cervix investigated by repetitive CT-examinations. *Radiother Oncol* 2001;60:273–80.
21. Baltas D, Kolotas C, Geramani K, et al. A conformal index (coin) to evaluate implant quality and dose specification in brachytherapy. *Int J Radiat Oncol Biol Phys* 1998;40:515–24.
22. International Commission on Radiation Units and Measurements (ICRU). Dose and volume specification for reporting interstitial therapy. *ICRU Report 58*. Bethesda, MD: ICRU, 1997.
23. Sanchez-Nieto B, Nahum AE. The delta-TCP concept: a clinically useful measure of tumor control probability. *Int J Radiat Oncol Biol Phys* 1999;44:369–80.
24. Webb S, Nahum AE. A model for calculating tumor control probability in radiotherapy including the effects of inhomogeneous distributions of dose and clonogenic cell density. *Phys Med Biol* 1993;38:653–66.
25. Burman C, Kutcher GJ, Emami B, et al. Fitting of normal tissue tolerance data to an analytic function. *Int J Radiat Oncol Biol Phys* 1991;21:123–35.
26. Kutcher GJ, Burman C, Brewster L, et al. Histogram reduction method for calculating complication probabilities for three-dimensional treatment planning evaluations. *Int J Radiat Oncol Biol Phys* 1991;21:137–46.
27. Sanchez-Nieto B, Nahum AE. Bioplan: software for the biological evaluation of radiotherapy treatment plans. *Med Dosim* 2000;25:71–6.
28. Dale E, Hellebust TP, Skjönsberg A, et al. Modeling normal tissue complication probability from repetitive computed tomography scans during fractionated high-dose-rate brachytherapy and external beam radiotherapy of the uterine cervix. *Int J Radiat Oncol Biol Phys* 2000;47:963–71.